2. Transverse Wave Loads on a Ship in Waves

(Part I, Part II, and Part III)

Kunio GODA*, *Member*

(From J.S.N.A. Japan, Vol. 121, Jnne 1967, Vol. 123, June 1968, and Vol. 126, December 1969.)

Summary

This paper deals with the hydrodynamic pressures acting on the ship hull in waves from the viewpoint of transverse strength of ships. Experimental investigations are made, in Part I, on the hydrodynamic pressures on the midship of T2 tanker model in regular head waves. In Part II, are presented results of calculations and experiments of the hydrodynamic pressures on the fore body of the same model. Calculations are carried out by using Tasai's method based on the strip theory. As the first step to obtain standard loads for transverse strength calculation, the joint probability distribution of the hydrodynamic pressures on the side and on the bottom of ships, in irregular waves is discussed in Part III.

Part I. Hydrodynamic Pressures on the Midship

1. Introduction

One of the most important problems in ship structural design is determination of the wave loads acting on the hull. While our knowledge on the longitudinal wave bending moments has been remarkably improved, few investigations have been carried out, from the viewpoint of transverse strength of ships, on the hydrodynamic pressures acting on the hull in waves. Akita and Ochi[1], Tasaki[2] measured the pressures on the bottom of a ship model going in regular head waves. Porter[3], Paulling[4], and Huang[5] reported measurements and calculations of the pressures on cylinders and on a shiplike model oscillating in free surface. At the 11th ITTC 1966, Hoffman[6] presented a interm report of measurements of the pressures on several sections of T2 Tanker model in regular waves. Data of full scale measurements on the Ocean Vulcan[7] and the Ginga-maru[8] are also available.

In Part I investigations of the hydrodynamic pressures on the bottom and the side of a model at the midship in waves are described from the transverse strength viewpoint. Model tests were conducted in regular head waves with T2-SE-A1 tanker model. Approximate calculations of the pressures on the bottom were carried out by means of the strip theory and compared with experimental results.

2. Description of Experiments

The model tests were conducted in the Mejiro No. 1 Ship Experiment Tank**, Ship Research Institute. The wooden model of T2-SE-A1 tanker was used, whose principal particulars are listed in Table 1.1. Bilge keels were not attached to the model. The model was self-propelled under full load and even keel condition in regular head waves having a wave length of 75, 100, 125 and 150% of model length respectively. The wave heights were controlled to 10 cm throughout the experiments.

The followings were measured:

(1) Hydrodynamic pressures on the hull at the midship.

* Ship Structure Division, Ship Research Institute.

** At present belongs to the Shipbuilding Research Center of Japan.

(2) Relative water level with respect to the hull at the midship side.
(3) Ship motions; pitching, heaving, and surging.
(4) Wave heights at a point in front of the towing carriage.

In Fig. 1.1 locations of pressure gages are shown. The pressure gages are electric capacitive type, and diameter of pressure sensing diaphragm is 30 mm. The wave heights were measured by the sonic wave probe located in front of the towing carriage, moving together with the carriage. And the relative water level was measured also by the sonic wave probe which was attached to the ship side as shown in Fig. 1.1. The speed of the towing carriage was taken as the model speed.

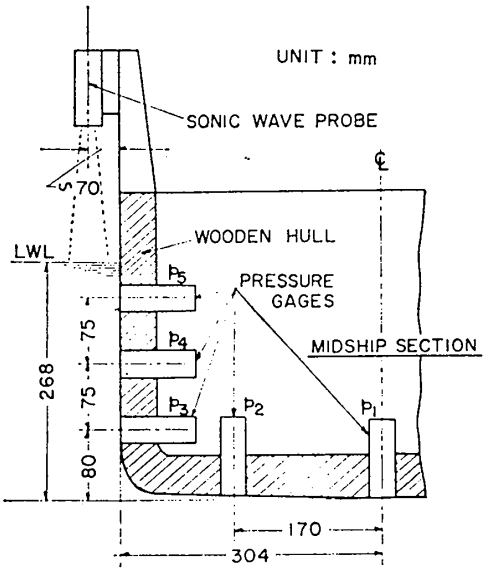

Fig. 1.1 Arrangement of Pressure Gages.

3. Results of Experiments

3.1 Pitching and Heaving

In Fig. 1.2 test results of pitching and heaving are shown, together with Fukuda's calcu-

Table 1.1 Particulars of Model.

Ship's Type	T2-SE-A1 Tanker
Length between Perpendiculars, L	4.500 m
Breadth moulded, B	0.608 m
Depth moulded, D	0.351 m
Draft, d	0.268 m
Block Coefficient, C_B	0.74
Displacement (fresh water), Δ	543 kg
Longitudinal Gyradius (about C.G.), κ	0.236 L
Longitudinal Center of Buoyancy forward of midship	0.004 L =18 mm

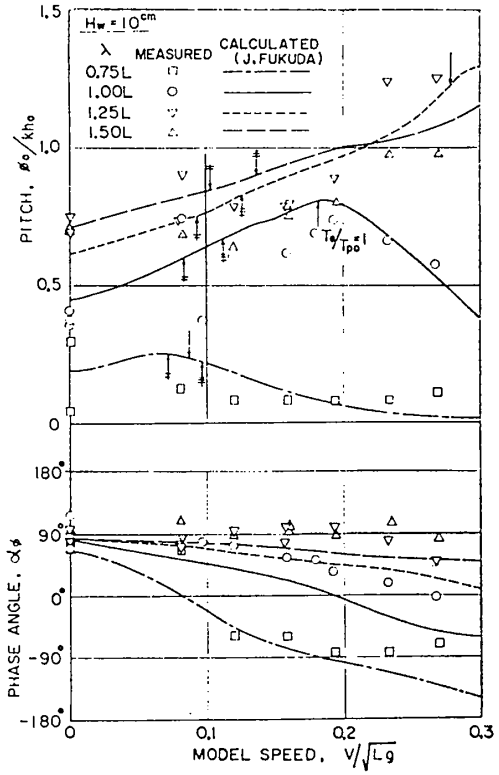

Fig. 1.2(a) Pitching Motions.

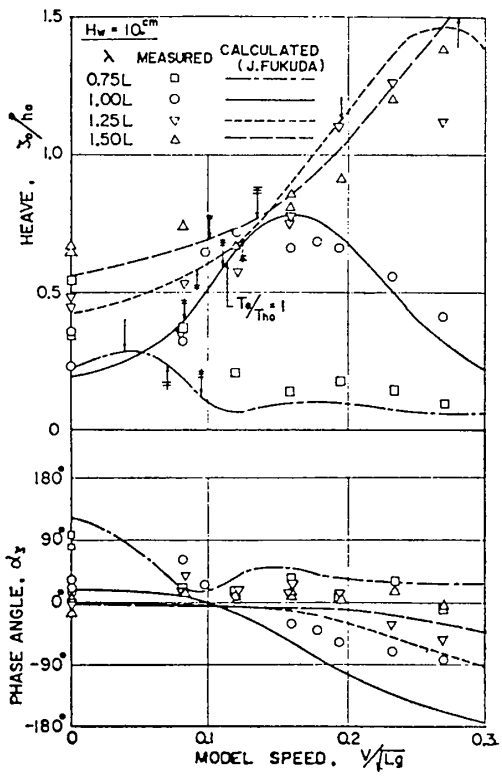

Fig. 1.2(b) Heaving Motions.

lated values by the strip theory[9]. The test results are presented in the forms of dimensionless amplitudes ϕ_0/kh_0 and ζ_0/h_0 and the phase angle of motions between motions and wave α_ϕ, α_ζ, where ϕ_0 is the amplitude of pitching, ζ_0 the amplitude of heaving, h_0 the amplitude of wave, $k=2\pi/\lambda$ the wave number, λ the wave length, L the ship length. The abscissa is model speed in term of Froude number $V/\sqrt{Lg}$. On definition of the phase angle, refer to Eqs. (1.1), (1.2) and (1.3) in chapter 4, Part I.

The heaving were measured at midship not at the center of gravity of the model, but the calculated value of heaving refer to the center of gravity. However, the center of gravity, being located 0.004 L(=18 mm) forward of midship, may be considered to be nearly at the midship.

Arrows, in Fig. 1.2, show the model speed at which the period of encounter T_e is equal to the natural period of pitching T_{p0} and heaving T_{h0}. These natural periods were obtained by free oscillation test in still water at zero speed. Vossers et al.[10] gave upper limit of model speed over which the side wall influence exists. Thislimit is indicated by the three-feather arrow, while the model speed corresponding to $\omega_e V/g=1/4$ is indicated by the two-feather arrow, ω_e being the circular frequency of encounter.

From Fig. 1.2, it can be said that the calculated values by the strip theory agree good with the experimental results.

3.2 *Hydrodynamic Pressure and Relative Water Level*

Examples of oscillograph records of the pressures and the relative water level are shown in Fig. 1.3. When the ship speed was not zero, high frequency ripples due to hull vibration induced by the electric motor on board for self propulsion were superposed on fundamental records.

The results of the hydrodynamic pressures and the relative water level are given in Fig. 1.4. These are presented in the form of dimensionless amplitude $p_0/\rho g h_0$ and $\hat{h}_0/h_0$, where p_0 is amplitude of the hydrodynamic pressure, ρ the density of water, g the acceleration of gravity, $\hat{h}_0$ the amplitude of the relative water level. The pressures at five locations are denoted by $p_1, p_2, \cdots, p_5$ as shown in Fig. 1.1. The hydrostatic pressure in still water are taken as zero reference. Arrows in the figures show the significant model speeds the same as explained in the previous section.

4. Analysis of Pressures on Bottom

By the strip theory[11] we calculate the vertical forces acting on the unit length of the hull at midship and then compare the values obtained by dividing the calculated vertical forces by model breadth (to be called the mean bottom pressure) with the test results of the hydrodynamic pressure on the bottom.

Consider the case when the ship goes for-

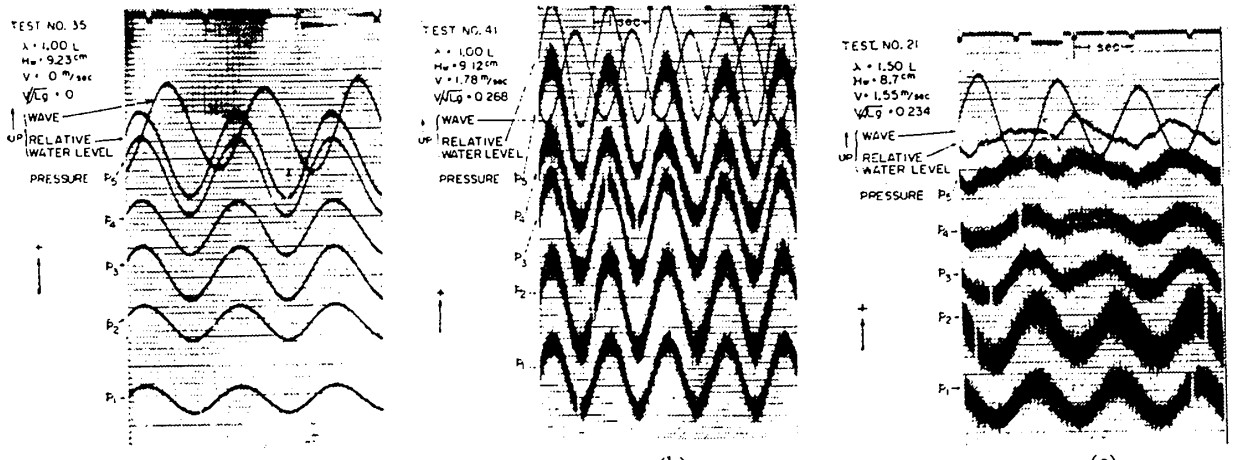

(a) (b) (c)

Fig. 1.3 Examples of Oscillograph Records.

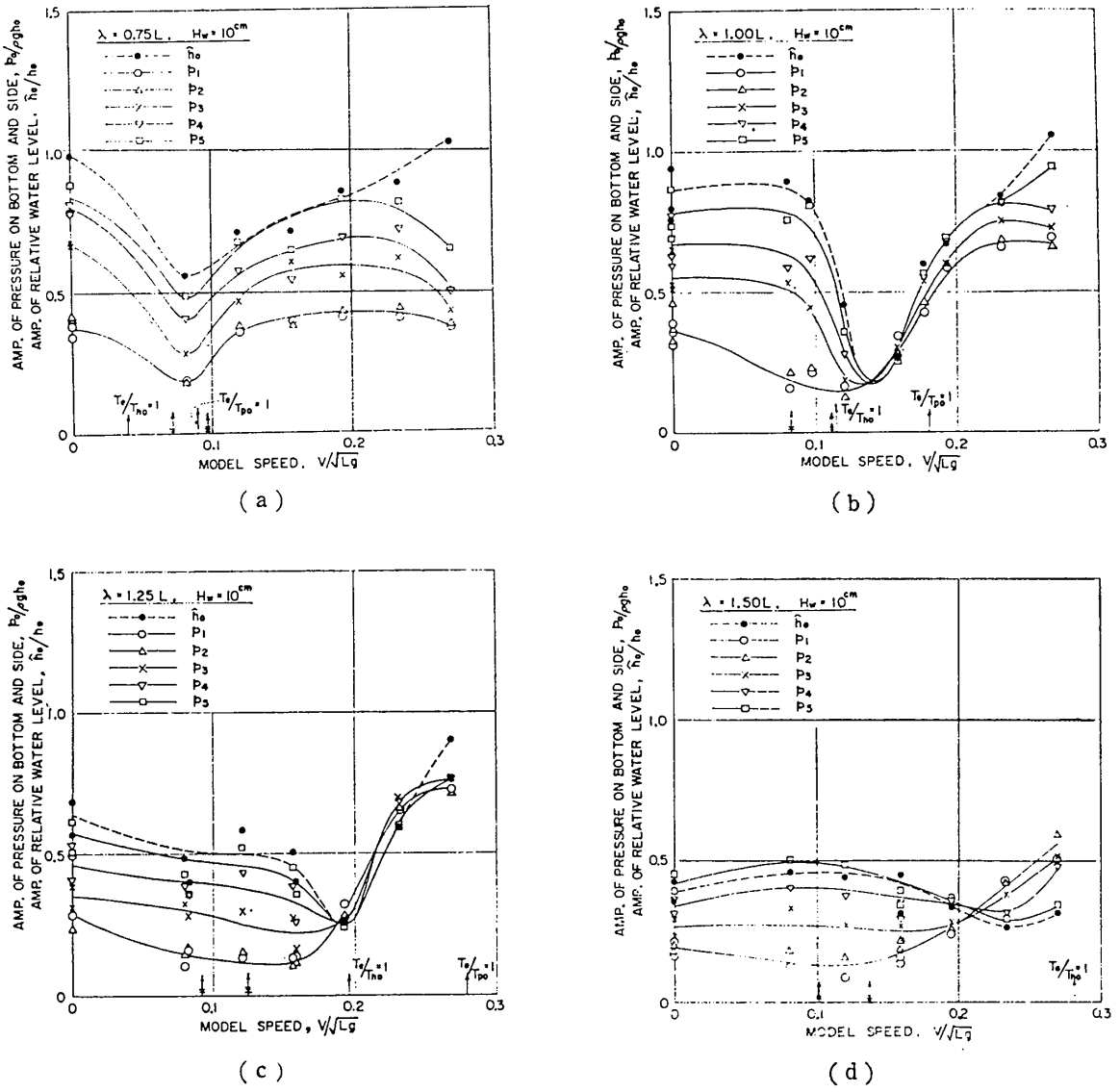

Fig. 1.4 Test Results of Hydrodynamic Pressures on Hull and Relative Water Level with Respect to Hull, at Midship.

ward with a constant speed V in regular head waves. As shown in Fig. 1.5, the co-ordinate system $O-XYZ$ fixed to the space is employed such that the XY-plane coincide with the still water surface and the Z-axis indicates the upward direction perpendicular to the still water surface. The co-ordinate system G_0-xyz fixed to the ship is chosen such that the origin locates at the center of gravity G_0 of the ship, the x-axis points out ahead the ship and z-axis upwards. The surface elevation h of regular head waves encountered the ship is

$$h=h_0\cos(kx+\omega_e t) \qquad (1.1)$$

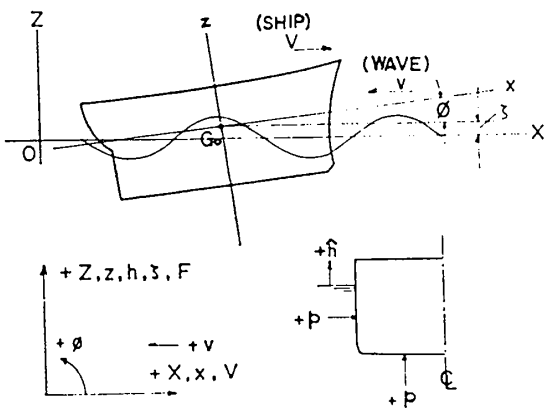

Fig. 1.5 Co-ordinate System.

And heaving ζ and pitching ϕ are

$$\zeta=\zeta_0 \cos(\omega_e t+\alpha_\zeta) \tag{1.2}$$

$$\phi=\phi_0 \cos(\omega_e t+\alpha_\phi) \tag{1.3}$$

where ω_e is the circular frequency of encounter. According to the strip theory, the force acting on the unit length of the ship at point x of the co-ordinate system fixed to the ship at an arbitrary time t is expressed as

$$\frac{dF}{dx}=\frac{dF_1}{dx}+\frac{dF_2}{dx}+\frac{dF_3}{dx} \tag{1.4}$$

where

$$\frac{dF_1}{dx}=-2pgy(Z-h_e) \tag{1.5}$$

$$\frac{dF_2}{dx}=-N(\dot{Z}-\dot{h}_e) \tag{1.6}$$

$$\frac{dF_3}{dx}=-\frac{d}{dt}\{u(\dot{Z}-\dot{h}_e\}) \tag{1.7}$$

and Z is the displacement of the ship's section with respect to the space co-ordinate system, y the half breadth of the water plane, u the added mass of the section and N the damping coefficient of the section. And the following relations exists:

$$Z=\zeta+x\phi \tag{1.8}$$

$$\dot{Z}=\dot{\zeta}+x\dot{\phi}-V\phi \tag{1.9}$$

$$\ddot{Z}=\ddot{\zeta}+x\ddot{\phi}-2V\phi \tag{1.10}$$

$$\frac{du}{dt}=-V\frac{du}{dx} \tag{1.11}$$

Assuming that the effective elevation of the wave h_e at the point of the ship is equal to the elevation of sub surface at the depth $Z=-\xi_m$, ξ_m being the mean draft of the section, then the effective elevation of the wave is expressed as

$$h_e=h_0 e^{-k\xi_m}\cos(\omega_e t+kx) \tag{1.12}$$

Since the section under consideration is the midship section, located in the parallel body, $2y=B$, $du/dx=0$ and $x\fallingdotseq 0$. From these relation and Eqs. (1.8) through (1.11), Eqs. (1.5) through (1.7) become

$$\frac{dF_1}{dx}=-\rho gB\zeta+\rho gBh_e \tag{1.13}$$

$$\frac{dF_2}{dx}=-N\dot{\zeta}+NV\phi+N\dot{h}_e \tag{1.14}$$

$$\frac{dF_3}{dx}=-u\ddot{\zeta}+2uV\dot{\phi}+u\ddot{h}_e \tag{1.15}$$

where B is the breadth of the ship.

The mean pressure on bottom p_m is

$$p_m=\frac{1}{B}\left(\frac{dF_1}{dx}+\frac{dF_2}{dx}+\frac{dF_3}{dx}\right)$$
$$=p_{m0}\cos(\omega_e t+\alpha_{pm}) \tag{1.16}$$

And the relative water level h is

$$\hat{h}=h-\zeta=\hat{h}_0\cos(\omega_e t+\alpha_{\hat{h}}) \tag{1.17}$$

In Fig. 1.6, the dimensionless amplitudes of the mean pressure on the bottom, i.e. $\bar{p}_{m0}=p_{m0}/\rho gh_0$, and their phase angle α_{pm} are presented by the solid line; those of the relative water levels, i.e. $\bar{\hat{h}}=\hat{h}_0/h_0$, and their phase angle $\alpha_{\hat{h}}$ by the broken line. And they are compared with the experimental results of the amplitudes of the bottom pressure p_1, p_2 and the phase angle of p_1, i.e. α_{p1}.

For ζ and ϕ necessary for the above calculations, Fukuda's calculations[9] shown in Fig. 1.2 and for u and N, Tasai's values[12] were adopted.

It is clear from Fig. 1.6, that good agreements between calculated and experimental results of both amplitude and phase angle of the pressure on the bottom is found. As for the relative water level, there exists discrepancy between calculations and test results. It is considered to be due to distorsion of the waves in the vicinity of the model and also due to the wave generated by motions of ship itself.

The vertical force acting on the unit length of the ship consists of several force components given in relations (1.13), (1.14), and (1.15).

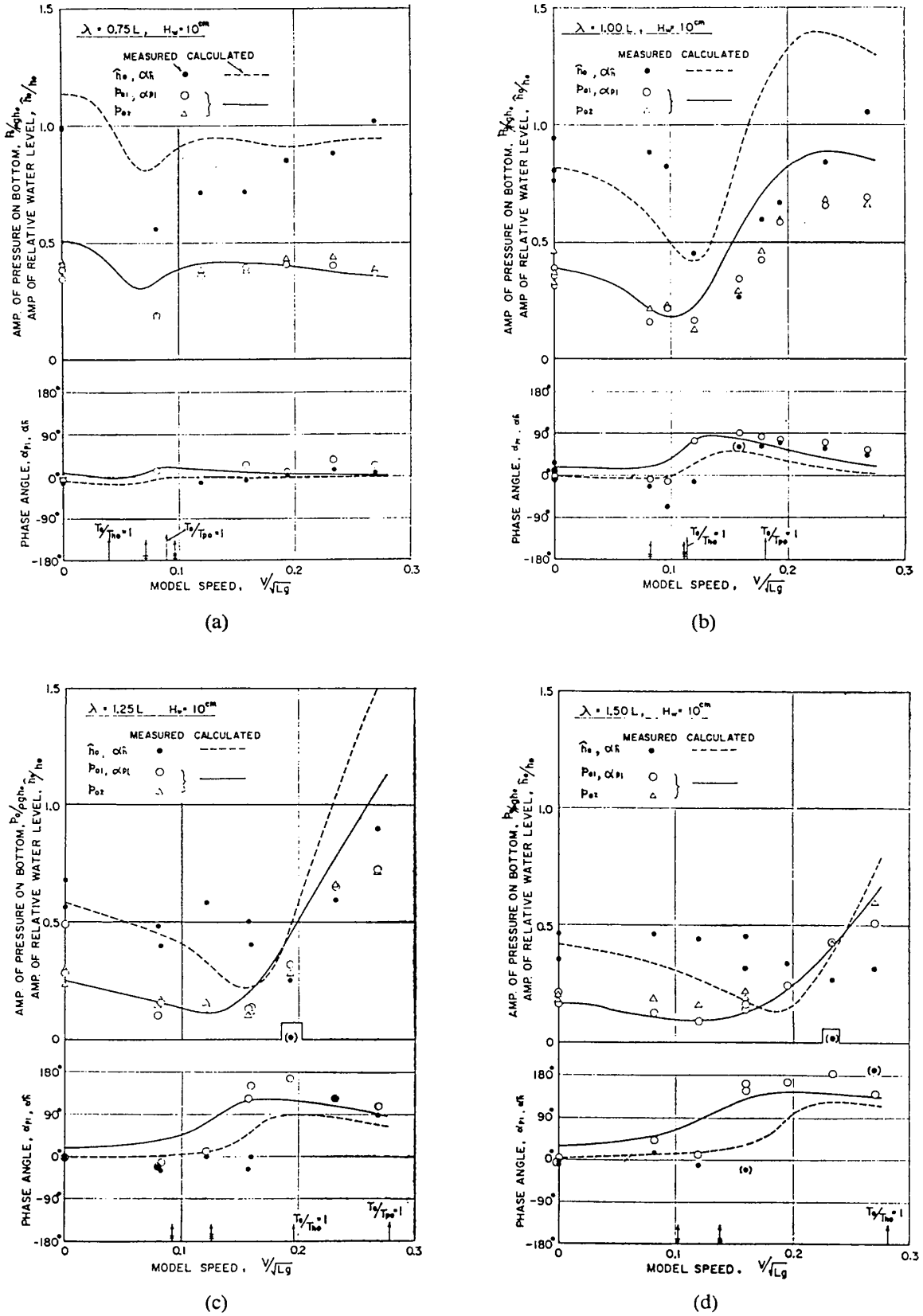

Fig. 1.6 Hydrodynamic Pressures on Bottom and Relative Water Level with Respect to Hull, at Midship.

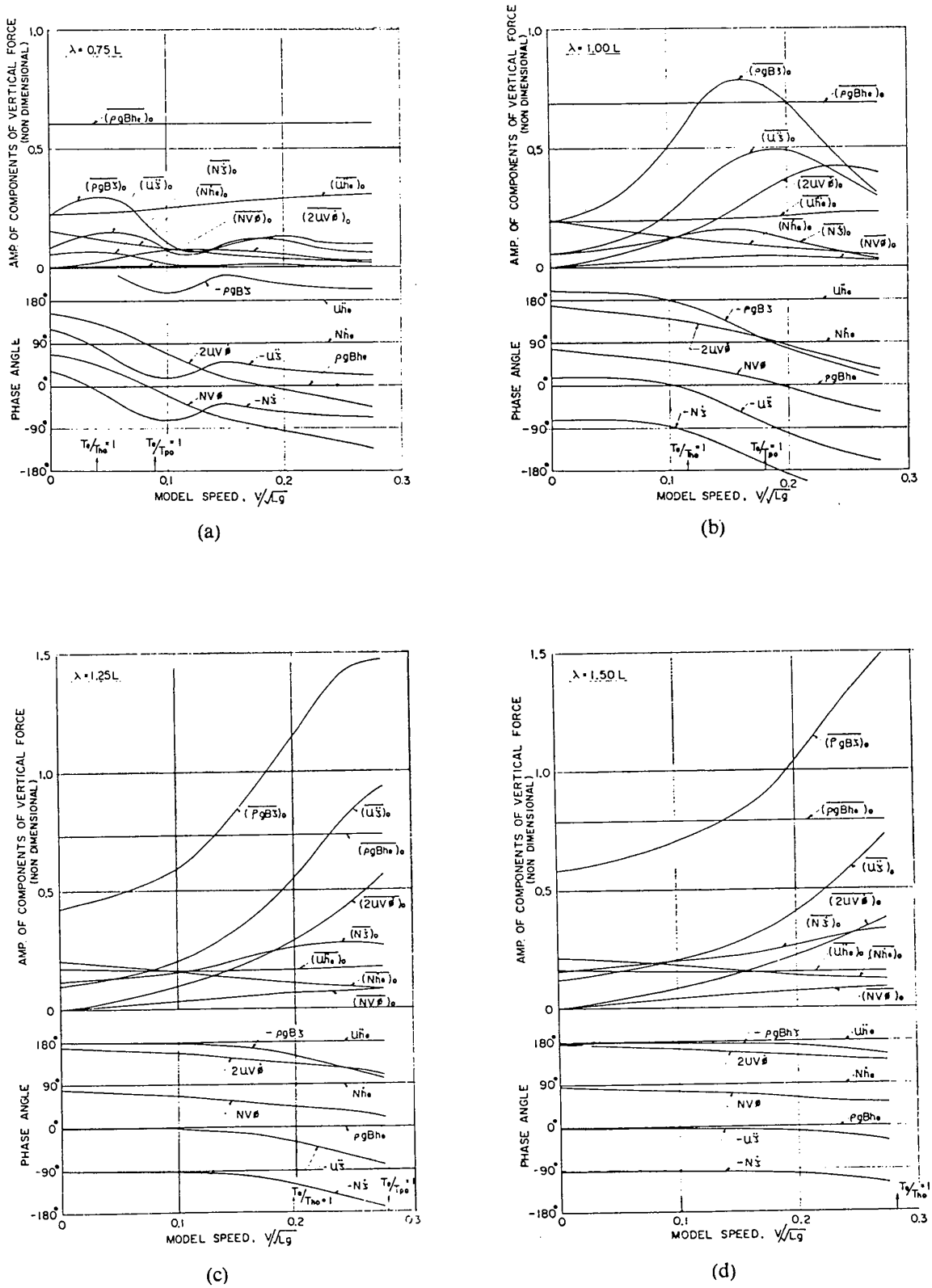

Fig. 1.7 Components of Vertical Force on Midship Section.

In Fig. 1.7, these components are shown in dimensionless forms which are value obtained by dividing the components by $\rho g h_0 B$. For example, $\overline{(\rho g B\zeta)_0}$ is amplitude of $\rho g B\zeta / \rho g h_0 B$. Among these components, the components $\rho g B h_e$, $\rho g B\zeta$ and $u\dot{\zeta}$ are predominant.

5. Conclusions

In this part, the hydrodynamic pressures on the bottom and on the side of the ship at midship are studied by the model tests.

Some approximate calculations of the pressures on the bottom were carried by means of the strip theory and compared with the experimental results. Good agreement between the calculations and the experimental results was found.

This calculation would be impossible except for a body plan which is neatly rectangular, also it would be impracticable for the pressure distribution on the bottom being far from uniform. When, however, it is considered that the body plan of many merchant ships is usually rectangular and calculation of the transverse strength is little affected by slight unevenness of the pressure distribution on the bottom, the above calculation may be sufficiently practical.

Appendix to Part I. Note on the Pressure Gage

A.1 *Problems of the Pressure Gage*

In the measurements of the hydrodynamic pressures on the ship model, the following problems should be considered: (1) Sensitivity; (2) Effect of temperature change; (3) Effect of acceleration.

(1) Sensitivity. In the case of, for example, test of 4.5 m model in waves of 10 cm wave height, the hydrodynamic pressure amplitudes are several grams per square centimeter. The pressure gages should be sensitive enough to measure such low pressures.

(2) Effect of temperature change. In the measurements of the pressures by means of the pressure gages which use the diaphragm mounted with wire strain gages, oscillograph records often showed considerable amount of drift. The drift was considered to be caused by temperature change.

(3) Effect of acceleration. The pressure gages move together with the ship model. Inertia force induced by acceleration of the ship model motion on the pressure sensing mechanism is not so small as to be neglected in comparison with the external pressure. The effect of acceleration should be eliminated.

A.2 *Pressure Sensing Mechanism of the Pressure Gage*

Ready-made pressure gages which satisfied above-mentioned requirements were not found. Then, new pressure gages were made specially for the measurements described in this report. In Fig. A.1 the sectional plan of the pressure gage is shown. Clearance between the electrode and the diaphragm changes due to pressure acting on the diaphragm. Change of electric capacity caused by that of clearance is detected by a amplifier.

A.3 *Diaphragm*

The diaphragm which was made of phosphor bronze was 0.05 mm in thickness and 30 mm in diameter. This circular plate was soldered to a steel ring. Procedure of soldering was as follows: Solder was spread on the

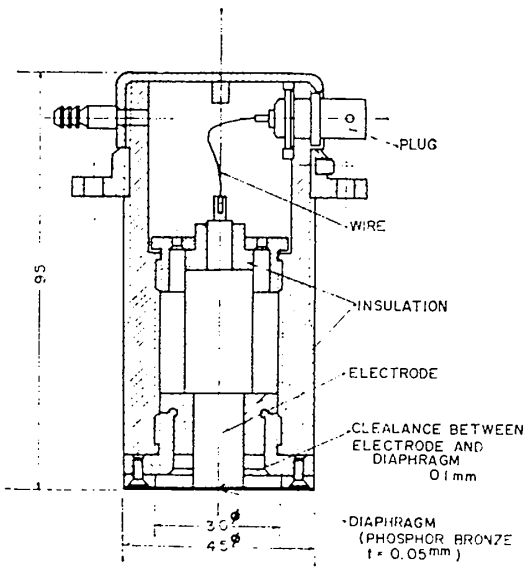

Fig. A.1 Sectional Plan of Pressure Gage.

soldering surface of the steel ring and of the diaphrag mseparately. Next, the diaphragm and the steel ring were heated at about 250°C. Then, these were lapped keeping that temperature. Finally, these were cooled down quickly. Thus the diaphragm was soldered to the steel ring with tension due to difference of expansion coefficients of steel and phosphor bronze.

Assuming that the above-mentioned diaphragm is a circular plate in tension with built-in edge under uniform pressure, deflection of center of the diaphragm δ is given by

$$\frac{\delta}{\delta_0}=\frac{16}{k^2}\left[\frac{2\{I_0(0)-I_0(k)\}}{kI_1(k)}+1\right] \quad (1a)^*$$

$$k^2=\frac{Ta^2}{D} \quad (2a)$$

where δ_0 is deflection of the diaphragm at center in case of zero tension, I_0 and I_1 are modified Bessel function of zero and first order, $D=Et^3/12(1-\nu^2)$, T is tension per unit length of circumference, a is radius of the circular plate, t is plate thickness, and ν is Poissons ratio.

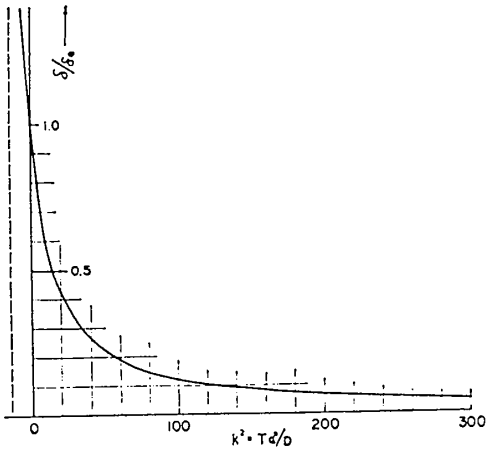

Fig. A.2 Defletion of Pressure Gage Diaphragm, at Center.

Graph of Eq. (1a) is shown in Fig. A.2. Assuming, for example, that melting temperature of solder is 180°C, room temperature is 20°C, and linear thermal expansion coefficients of steel and phosphor bronze are 1.12×10^{-5} and 1.68×10^{-5} respectively, then k^2 becomes 1.20×10^3 and δ/δ_0 0.0121. In the vicinity of the k^2 value slope of δ/δ_0-curve is very small: This means that the effect of temperature change on deflection of the plate is very small.

A.4 *Results of Performance*

No drift of oscillograph records was found during the test. However, some unsteadiness of sensitivity was found. In order to remove error due to this unsteadiness, calibration was frequently carried out.

* Calculation for the circular plate in compression is shown in "Plates and Shells" by Timoshenko.

Part II. Hydrodynamic Pressures on the Fore Body

1. Introduction

In Part I are described experimental studies of the hydrodynamic pressures on the midship, using the T2 tanker model. Just before the studies described in Part I were reported, Tasai had presented a method of calculation of the hydrodynamic pressures on the hull based on the strip theory. Then author calculated the hydrodynamic pressures on the midship of T2 tanker according to Tasai's method and compared the calculations with experimental results. This work[14] was presented at the meeting of the Society of Naval Architects of West Japan in February 1968. Author consecutively carried out investigations of the hydrodynamic pressures acting on the fore body of the ship using the same model. Results of investigations are shown in this part.

2. Method of Calculation of the Hydrodynamic Pressures

Theory for calculation of the hydrodynamic pressures is given in this chapter. The co-ordinate systems are employed as shown in Fig. 1.5; Explanation of those are given in Chapter 4, Part I. And the co-ordinate system for the section contour of the hull is shown in Fig. 2.1.

The hydrodynamic pressures on the hull surface consists of the following components:

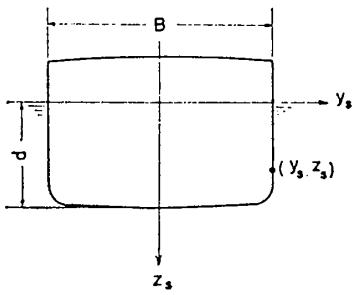

Fig. 2.1 Coordinate System for Section Contour.

(1) Hydrodynamic pressure due to the motion in still water, $P_{(1)}$.
(2) Hydrodynamic pressure due to reflection of waves from the body under restrained condition, $P_{(2)}$.
(3) Hydrodynamic pressure obtained from regular wave potential, $P_{(3)}$.

(1) Hydrodynamic pressure due to the motion in still water. When the cylindrical body, section of which is in Lewis form, oscillates on still water surface with circular frequency ω_e, the hydrodynamic pressure on the body will given by the following equation:

$$p=-\rho\frac{\partial\Phi}{\partial t}=\frac{\rho g\eta}{\pi}[(\Phi_c+S)\sin\omega_e t -(\Phi_s+E)\cos\omega_e t] \tag{2.1}$$

where ρ is the density of water, g the acceleration of gravity, η the amplitude of progressive wave generated by heaving, Φ_c and Φ_s are potential of the progressive wave, S and E are potential which satisfy the boundary condition. These potentials are given on Ref. 15.

Suppose that the two-dimentional body oscillates vertically with a small amplitude as given by

$$\zeta=\zeta_0\cos\omega_e t \tag{2.2}$$

we divide the hydrodynamic pressure into two parts, p_{aw} and p_{dw}. The former is in phase with $\ddot{\zeta}$ and the latter in phase with $\dot{\zeta}$. By putting as

$$\left.\begin{aligned} p_{aw}&=\rho g\zeta_0 p''_{aw}\cos\omega_e t\\ p_{dw}&=\rho g\zeta_0 p''_{dw}\sin\omega_e t,\end{aligned}\right\} \tag{2.3}$$

p''_{aw} and p''_{dw} will be obtained by

$$\left.\begin{aligned} p''_{aw}&=-\xi_B\frac{p_sB_0+p_cA_0}{A_0^2+B_0^2}\\ p''_{dw}&=-\xi_B\frac{p_sA_0-p_cB_0}{A_0^2+B_0^2}\end{aligned}\right\} \tag{2.4}$$

where $\xi_B=\omega_e^2B/2g$, $p_s=\Phi_s+E$, $p_c=\Phi_c+S$, B is breadth of the section, A_0 and B_0 are determined by section shape and ξ_B and given by Ref. 15).

Assuming that heaving ζ and pitching ϕ are expressed as

$$\left.\begin{aligned} \zeta&=\zeta_0\cos(\omega_e t+\alpha_\zeta)\\ \phi&=\phi_0\cos(\omega_e t+\alpha_\phi),\end{aligned}\right\} \tag{2.5}$$

the following relations exist:

$$\left.\begin{aligned} Z&=\zeta+x\phi\\ \dot{Z}&=\dot{\zeta}+x\dot{\phi}-V\phi\\ \ddot{Z}&=\ddot{\zeta}+x\ddot{\phi}-2V\dot{\phi}\end{aligned}\right\} \tag{2.6}$$

where Z is vertical displacement of the section at point x, V the ship speed.

The hydrodynamic pressure $p_{(1)}$ at point x is given by

$$p_{(1)}=-\rho gZ+\rho g\frac{p''_{dw}}{\omega_e}\dot{Z}+\rho g\frac{p''_{aw}}{\omega_e^2}\ddot{Z} \tag{2.7}$$

Substituting Eq. (2.6) into Eq. (2.7), we obtain

$$p_{(1)}=p_h+p_\phi+p_{hd}+p_{\phi d}+p_{\phi vd}+p_{ha}+p_{\phi a}+p_{\phi va} \tag{2.8}$$

where

$$\left.\begin{aligned} p_{\phi vd}&=-\rho g\zeta & p_\phi&=-\rho gx\phi\\ p_{hd}&=\rho g\frac{p''_{dw}}{\omega_e}\dot{\zeta} & p_{\phi d}&=\rho g\frac{p''_{dw}}{\omega_e}x\dot{\phi}\\ p_{\phi vd}&=-\rho g\frac{p''_{dw}}{\omega_e}V\phi & p_{ha}&=\rho g\frac{p''_{aw}}{\omega_e^2}\ddot{\zeta}\\ p_{\phi a}&=\rho g\frac{p''_{aw}}{\omega_e^2}x\ddot{\phi} & p_{\phi va}&=-2\rho g\frac{p''_{aw}}{\omega_e^2}V\dot{\phi}\end{aligned}\right\} \tag{2.9}$$

(2) Hydrodynamic pressure due to reflection of wave from the body under restrained

condition. Sub-surface elevation of regular head waves h_e is expressed as

$$h_e = h_0 e^{-kZ} \cos(kX + \omega t) \qquad (2.10)$$

where h_0 is the wave amplitude, $k = 2\pi/\lambda$, λ is the wave length, z is the depth from water surface, w is the circular frequency of wave. The sub-surface elevation with respect to the hull will be

$$h_e = h_0 e^{-hz_s} \cos(kx + \omega_e t) \qquad (2.11)$$

where ω_e is the circular frequency of encounter and Z_s is co-ordinate of the point on the hull. (Fig. 2.1) Hence orbital velocity and orbital acceleration of wave at point x are

$$\dot{h}_e = -h_0 \omega e^{-kz_s} \sin(\omega_e t + kx) \qquad (2.12)$$

$$\ddot{h}_e = -h_0 \omega^2 e^{-hz_s} \cos(\omega_e t + kx) \qquad (2.13)$$

The hydrodynamic pressure $p_{(2)}$ is given by the following equation:

$$p_{(2)} = p_{wd} + p_{wa} \qquad (2.14)$$

$$\left.\begin{aligned} p_{wd} &= -\rho g \frac{\rho''_{dw}}{\omega_e} \dot{h}_e \\ p_{wa} &= -\rho g \frac{p''_{aw}}{\omega_e^2} \ddot{h}_e \end{aligned}\right\} \qquad (2.15)$$

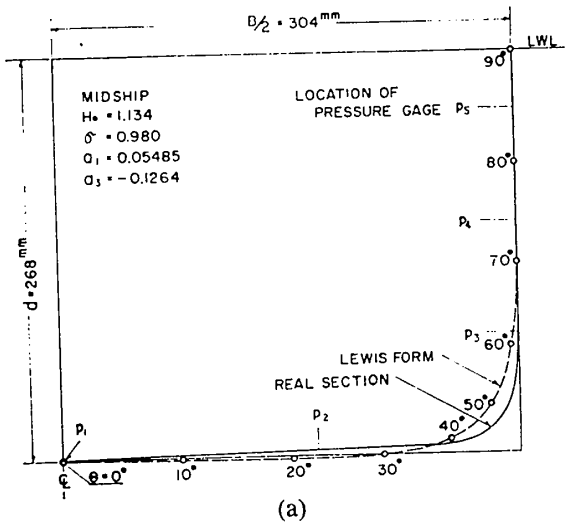

(a)

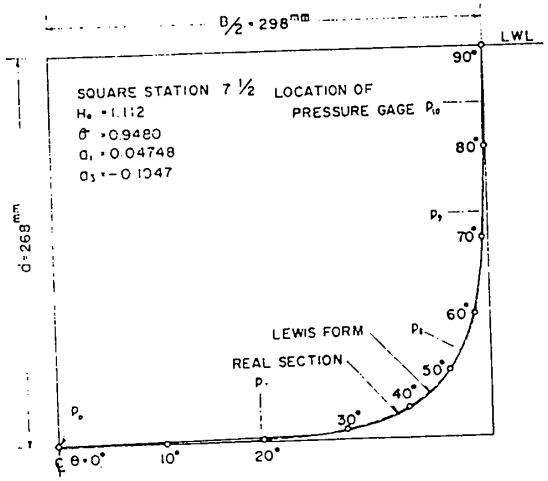

(b)

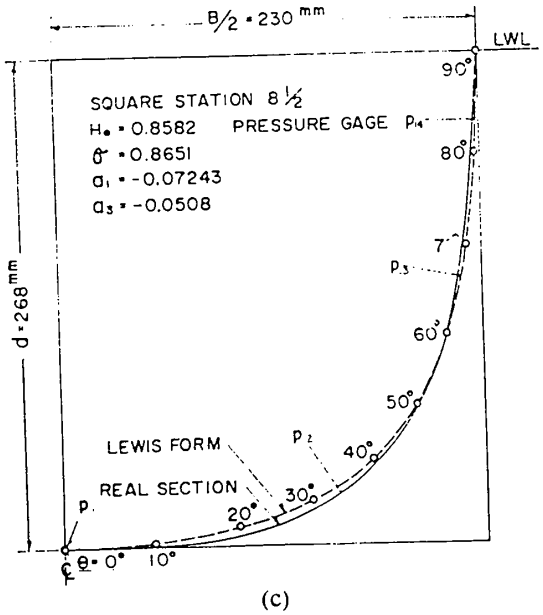

(c)

Fig. 2.2 Section Contours and Locations of Pressure Gages.

(3) Hydrodynamic pressure obtained from regular wave potential. This is given by

$$p_{(3)}=\rho g h_0 e^{-kz_s}\cos(\omega_e t+kx)=p_w \quad (2.16)$$

The hydrodynamic pressure acting on the hull in regular head waves is sum of above three components:

$$\begin{aligned} p&=p_{(1)}+p_{(2)}+p_{(3)}\\ &=p_h+p_\phi+p_{hd}+p_{\phi d}+p_{\phi vd}+p_{ha}\\ &\quad+p_{\phi a}+p_{\phi va}+p_{wd}+p_{wa}+p_w\\ &=p_0\cos(\omega_e t+\alpha p) \end{aligned} \quad (2.17)$$

3. Results of Calculation and Experiment

3.1 *Calculation*

Using the method of calculation in previous chapter, numerical calculation were carried out on the hydrodynamic pressures acting on square station 7½ and 8½ (0.25 L and 0.15 L from *F.P.*) of T2 tanker model the same as described in Part I. Section contours of S.S. 7½, S.S. 8½, and the midship are shown in Fig. 2.2. In the figures the real sections of the ship are shown by solid lines and Lewis forms, which are determined by the following equations, for the real sections are shown by broken lines:

$$\left.\begin{aligned} y_s&=M\{(1+a_1)\sin\theta-a_3\sin 3\theta\}\\ z_s&=M\{(1-a_1)\cos\theta+a_3\cos 3\theta\}\\ M&=\frac{B}{2}\Big/(1+a_1+a_3) \end{aligned}\right\} \quad (2.18)$$

The Lewis forms are used for the calculation. In Fig. 2.2 σ is the cross sectional area coefficient, a_1 and a_3 are determined by H_0 and σ, and $H_0=(B/2)/(d)$. Points for $\theta=0°$, $10°,\cdots,90°$ are shown by small circles in the figures.

Calculated results of the hydrodynamic pressure amplitudes at S.S. 7½ and S.S. 8½ are shown in Figs. 2.3 and 2.4. For comparison, the hydrodynamic pressure amplitudes at $\theta=0°$ and 90° at the midship are shown together in the figures. And broken lines shown the amplitudes of the relative water level with respect to the hull, and chain lines show the amplitudes of mean pressure on the bottom described in Part I. These calculated results of the pressures and the relative water levels are presented against the model speed in term of Froud number in the forms of dimensionless amplitude $p_0/\rho g h_0$ and $\hat{h}_0/h_0$, where p_0 is the amplitude of the hydrodynamic pressure, ρ is the density of water, g is the acceleration of gravity, $\hat{h}_0$ is the amplitude of the relative water level, and h_0 is the wave amplitude.

From Figs. 2.3 and 2.4, it can be said that the amplitudes of the hydrodynamic pressures on the fore body are larger than those of the midship; the amplitudes at S.S. 8½ are largest, and those at S.S. 7½ are larger than at the midship. This seems to be caused by the vertical motion $x\phi$. While the hydrodynamic pressure on the bottom are distributed almost uniformly at the midship as reported in Ref.[14], at S.S. 7½ the amplitude of the pressure on the bottom increases little by little from center to bilge part.

3.2 *Experiment*

In Figs. 2.5 and 2.6, are shown comparison of calculated and measured amplitudes of the hydrodynamic pressures at S.S. 7½ and S.S. 8½.

The model tests were carried out in the Meguro Model Basin of the Defense Agency. The model and the experiment procedure were the same as those described in Chapter 2, Part I. The hydrodynamic pressures were measured at locations denoted by P_6, P_7, ..., P_{14} as shown in Fig. 2.2.

From Figs. 2.5 and 2.6, it can be considered that good agreement between calculation and experimental results is found at S.S. 7½. However, certain amount of descrepancy is found between test results and calculation of the amplitudes of the hydrodynamic pressures on the S.S. 8½. This seems to be caused by the end effect.

4. Conclusions

In Part II are presented results of calculations and measurements of the hydrodynamic pressures on the fore body (Square Station

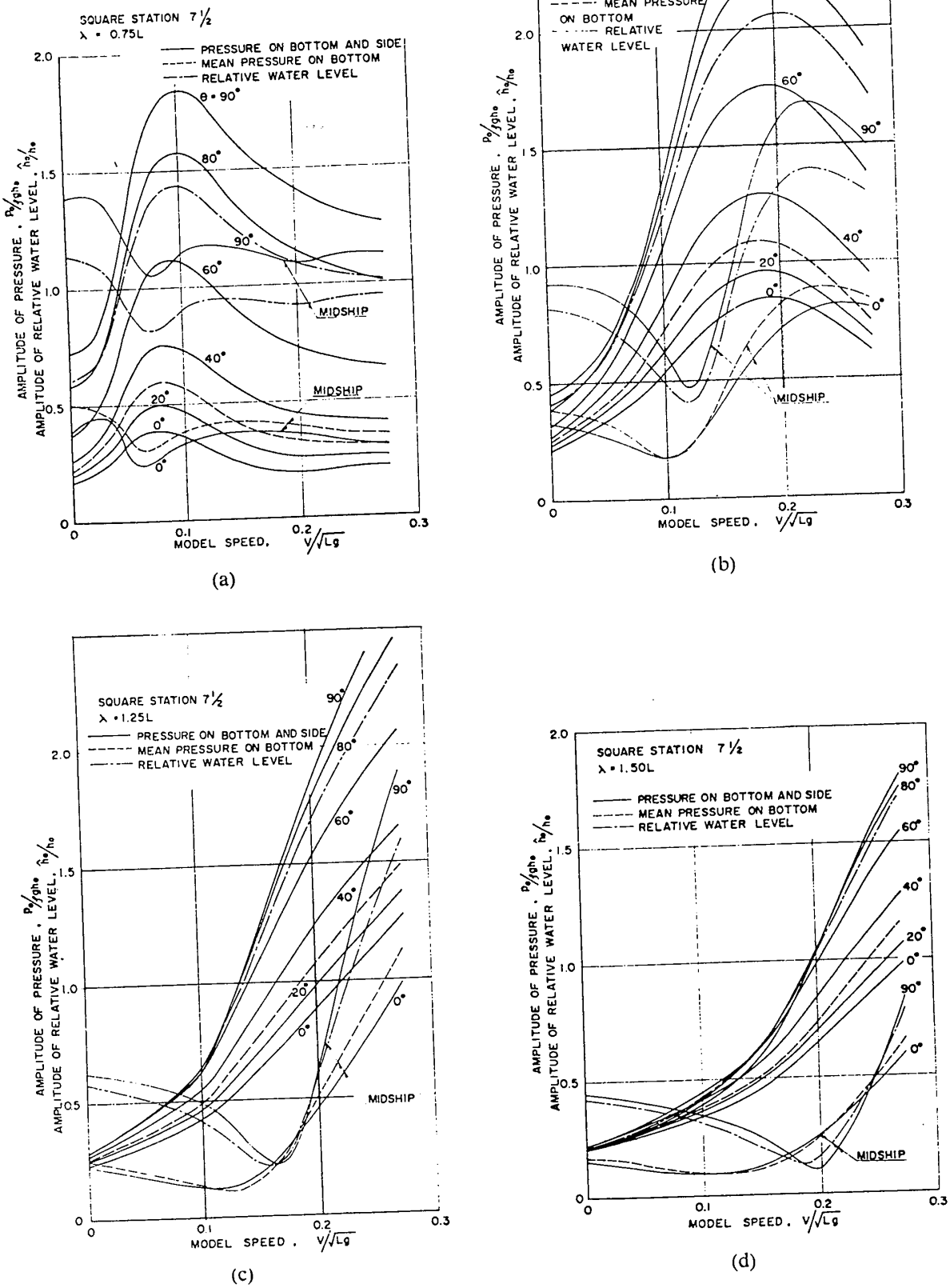

Fig. 2.3 Results of Calculation of Amplitudes of Hydrodynamic Pressures on Hull at Square Station $7^1/_2$.

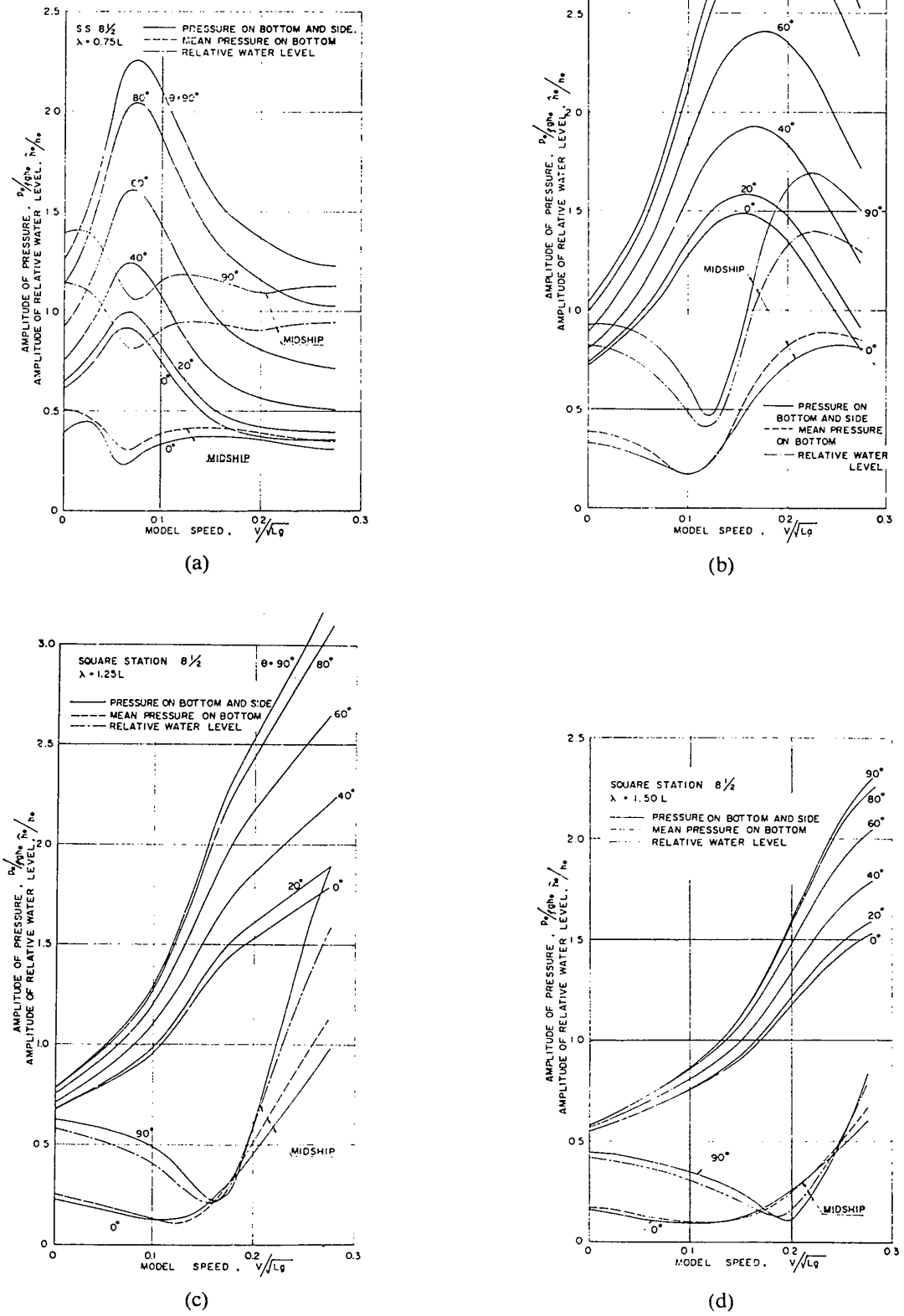

Fig. 2.4 Results of Calculation of Amplitudes of Hydrodynamic Pressures on Hull at Square Station $8^1/_2$.

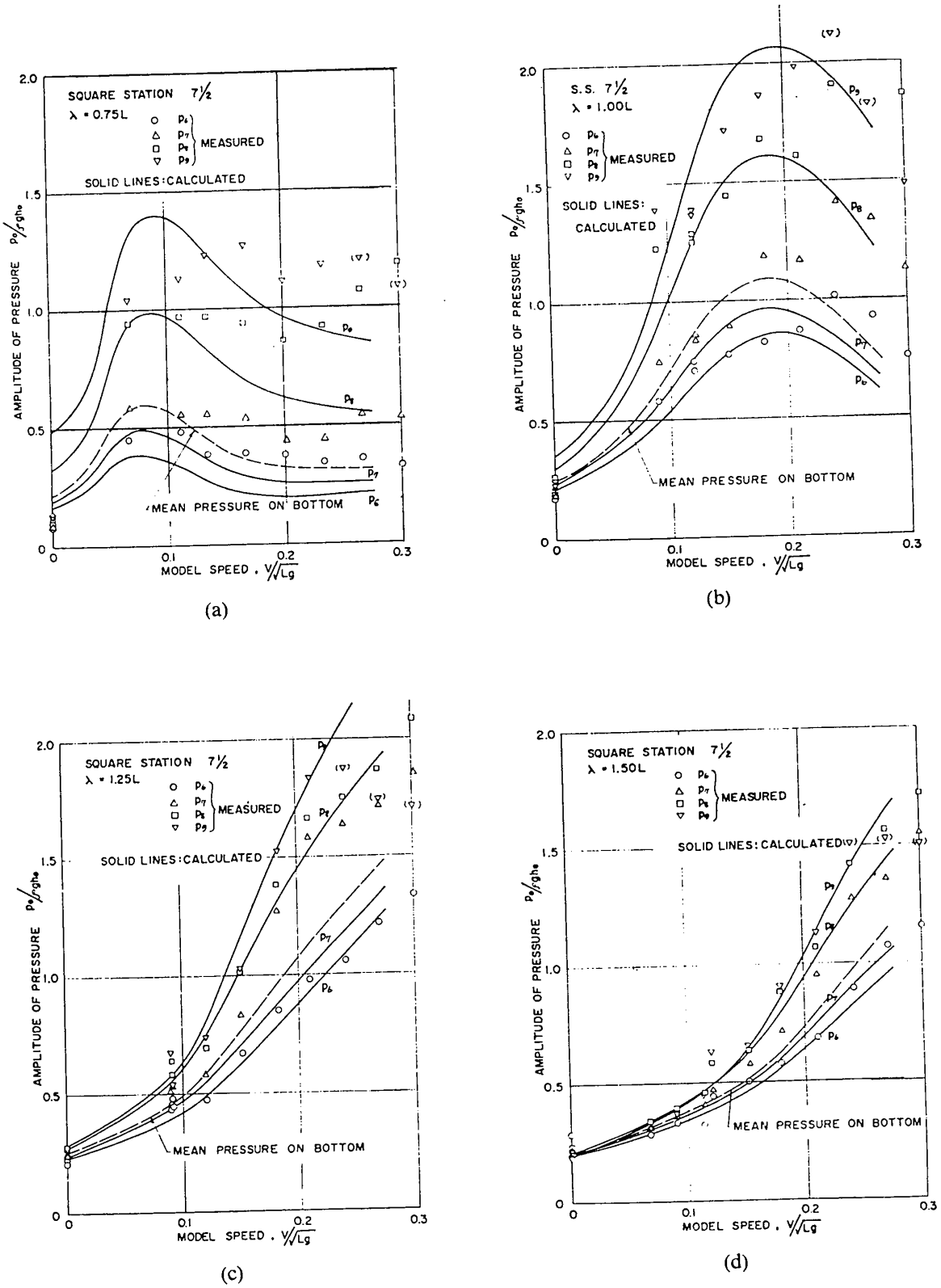

Fig. 2.5 Comparison of Calculated and Measured Amplitudes of Pressures on Hull at Square Station $7^1/_2$.

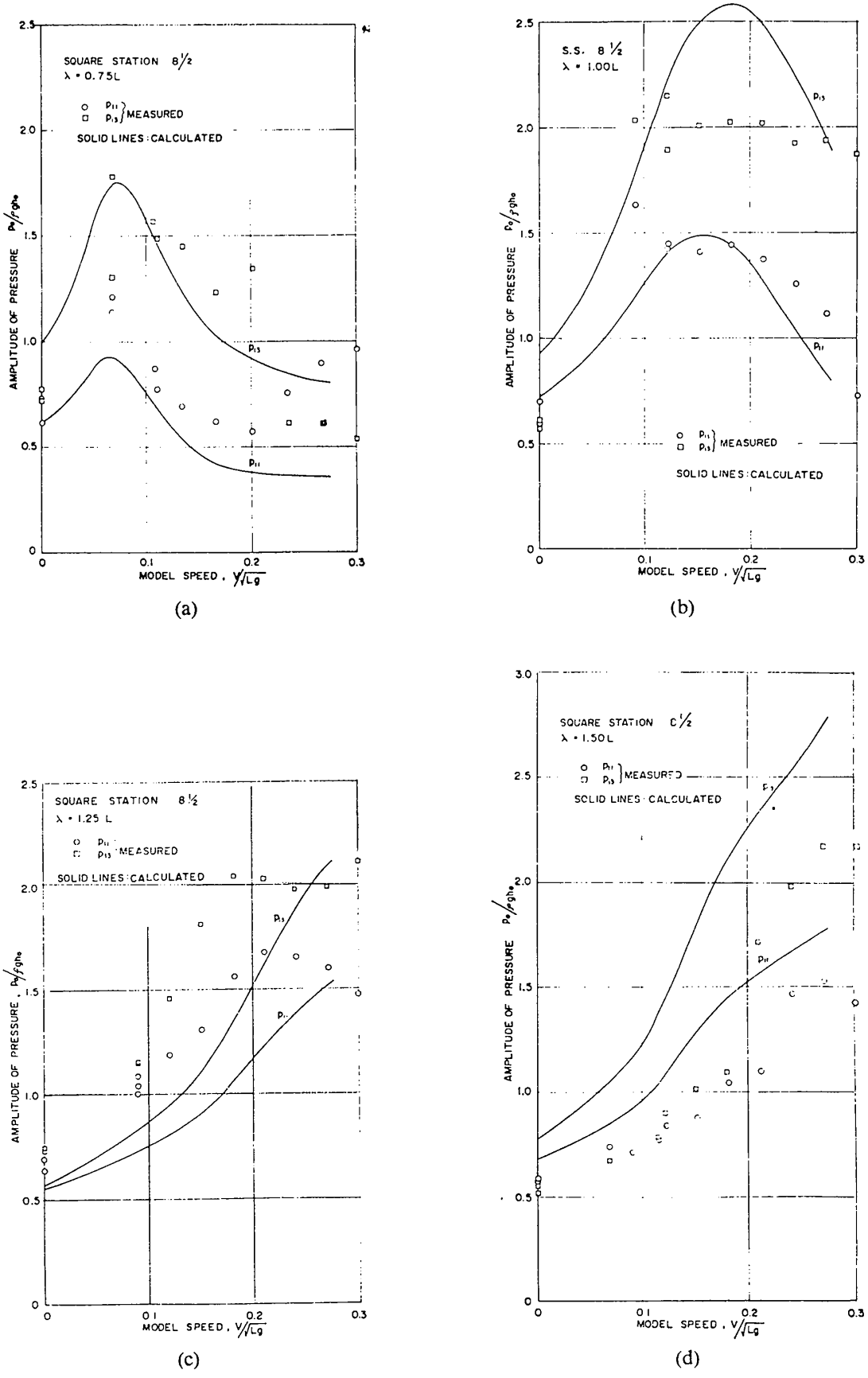

Fig. 2.5(a) Comparison of Calculated and Measured Amplitudes of Pressures on Hull at Square Station $8^1/_2$.

7½ and 8½) of T2 tanker model in regular head waves. From these results it may be concluded:

(1) Test results of the hydrodynamic pressure amplitude on S.S. 7½ coinside fairly well with the calculated values by means of the strip theory. However, certain amount of descrepancy between test results and calculations on S.S. 8½ is found.

(2) Amplitudes of the hydrodynamic pressures on the fore body are larger than those on the midship; those were larger in order of S.C. 8½, S.S. 7½, and the midship.

Part III. Pressure Distribution Along the Girth in Long-Crested Irregular Head Aeas

1. Introduction

In Parts I and II author dealt with the hydrodynamic pressures on the hull in regular head waves. In ocean waves the hydrodynamic pressures on the hull varies irregularly. Property of the irregularly changing pressures can be studied in statistical mean by the linear superposition principle. When we study the hydrodynamic pressures from the standpoint of transverse strength of ships, it is noted that spacial distribution of the pressure along the girth as well as on a point on the hull should be considered. In Part III, as the first step to obtain a standard loads for transverse strength calculation, the joint probability distribution of the hydrodynamic pressure on the ship side and on the bottom in irregular waves is discussed in order to study the statistical property of the spacial distribution of the pressure along the girth.

2. Joint Probability Distribution of the Hydrodynamic Pressures on the Ship Side and the Bottom

Consider the case when the ship goes forwards with constant speed in longcrested irregular head sea. In Fig. 3.1 are shown a sketch of the pressure distribution on a section at arbitrary time $t=t_1$. Symbols p_s, p_{b1} and p_{b2} denote the hydrodynamic pressures on points S, B_1 and B_2 respectively. Let the pressures p_s, p_{b1} and p_{b2} vary irregularly with time t as shown in Fig. 3.2. In regular waves, distribution of the pressure on the bottom is nearly uniform as shown in Parts I and II. Then it may be assumed that also in long-crested irregular head waves the pressure on bottom is uniformly distributed, and its magnitude is mean of p_{b1} and p_{b2} which is denoted by p_b. For the hydrodynamic presure on the ship side it may be assumed that the pressure vary linearly along the girth as shown in Fig. 3.1. Thus, distribution of the hydrodynamic pressure along the girth at $t=t_1$ can be determined by $p_s(t_1)$ and $p_b(t_1)$. Consequently, if the joint probability distribution of p_s and p_b is obtained, statistical property of spacial distribution of the pressure along the girth can be known.

Ocean wave have Gaussian property. The hydrodynamic pressures on the hull in ocean waves have also Gaussian property if it is

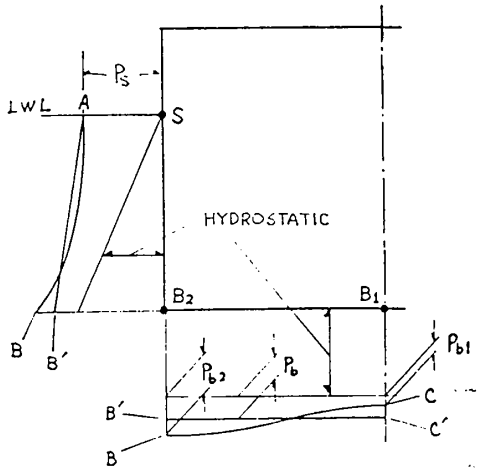

Fig. 3.1.

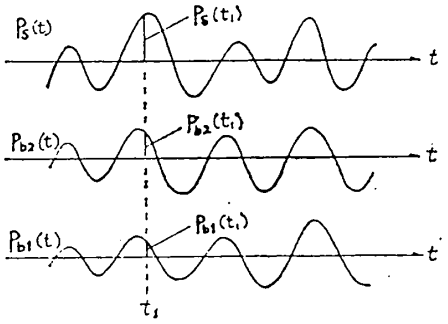

Fig. 3.2 Sketch of Simultaneous Records of the Hydrodynamic Pressures on the Hull.

assumed that the pressure amplitude is proportional to the wave height. Hence the joint probability distribution of the hydrodynamic pressure on the ship side $p_s(t_1)$ and on the bottom $p_b(t_1)$ is given by the following Gaussian distribution:

$$f\{p_s, p_b\}=\frac{1}{2\pi R_s R_b\sqrt{1-\rho^2}}e^{-\frac{1}{2}\phi(p_s,p_b)} \quad (3.1)$$

$$\phi(p_s, p_b)=\frac{1}{1-\rho^2}\left\{\frac{(p_s-m_s)^2}{R_s^2}-\frac{2\rho(p_s-m_s)(p_b-m_b)}{R_s R_b}+\frac{(p_b-m_b)^2}{R_b^2}\right\} \quad (3.2)$$

where ρ is the correlation coefficients of p_3 and p_b, R_s and R_b are the standard deviations of p_s and p_b respectively, m_s and m_b are the mean values of p_s and p_b which are zero because we consider the fluctuating pressures.

The standard deviations R_s and R_b are obtained by the followings:

$$R_s^2=\int_{-\infty}^{\infty}|H_{sw}(\omega)|^2 S_w(\omega)d\omega \quad (3.3)$$

$$R_b^2=\int_{-\infty}^{\infty}|H_{bw}(\omega)|^2 S_w(\omega)d\omega \quad (3.4)$$

where $H_{sw}(\omega)$ and $H_{bw}(\omega)$ are the response functions of p_s and p_b to the wave and $S_w(\omega)$ is the wave spectrum.

And ρ is given also from H_{sw}, $H_{bw}(\omega)$ and $S_w(\omega)$ as follows:

$$\rho=\frac{E(p_s, p_b)}{R_s\cdot R_b} \quad (3.5)$$

$$E\{p_s\cdot p_b\}=r_{bs}(\tau)_{\tau=0}=\int_{-\infty}^{\infty}S_{bs}(\omega)d\omega \quad (3.6)$$

$$S_{bs}(\omega)=H_{bw}(\omega)\cdot H_{sw}(\omega)\cdot S_w(\omega) \quad (3.7)$$

where $r_{bs}(\tau)$ is the cross-correlation function of p_s and p_b, $S_{bs}(\omega)$ is the croo-spectrum of p_s and p_b.

The response function $H(\omega)$ is complex number and expressed as follows:

$$H_{sw}(\omega)=C_s(\omega)+iQ_s(\omega) \quad (3.8)$$

$$H_{bw}(\omega)=C_b(\omega)+iQ_b(\omega) \quad (3.9)$$

Substituting Eqs. (3.8) and (3.9) into Eq. (3.6), we obtain

$$E\{p_s\cdot p_b\}=\int_{-\infty}^{\infty}\{C_s(\omega)\cdot C_b(\omega)+Q_s(\omega)\cdot Q_b(\omega)\}\cdot S_w(\omega)d\omega+i\int_{-\infty}^{\infty}\{C_s(\omega)Q_b(\omega)-C_b(\omega)\cdot Q_s(\omega)\}S_w(\omega)d\omega \quad (3.10)$$

In Eq. (3.10) the first term of right hand side is the even function of w and the second term is the odd function. Then

$$E\{p_s\cdot p_b\}=2\int_0^{\infty}\{C_s(\omega)\cdot C_b(\omega)+Q_s(\omega)\cdot Q_b(\omega)\}S_w(\omega)d\omega \quad (3.11)$$

3. Results of Calculation

According to the theory described in the previous chapter, numerical calculations have been carried out on the response function, the standard deviation, and correlation coefficient of the hydrodynamic pressures on the side and the bottom in longcrested irregular head seas for the typical ship forms of the oil tanker and the cargo ship. In table 3.1 are shown the principal particulars of the ship forms. Calculations were made for the hydrodynamic pressures on the midship and on

Table 3.1 Main Particulars of Ship Forms.

		Tanker	Cargo
Length/Breadth	L/B	6.00	7.00
Length/Draft	L/d	17.50	17.50
Block Coefficient	C_B	0.836	0.700
Midship Area Coefficient	$C_\otimes$	0.993	0.986
LCB from Midship (forward)		0.0336 L	0.005 L
Longitudinal Gyradius (about C.G)		0.245 L	0.250 L

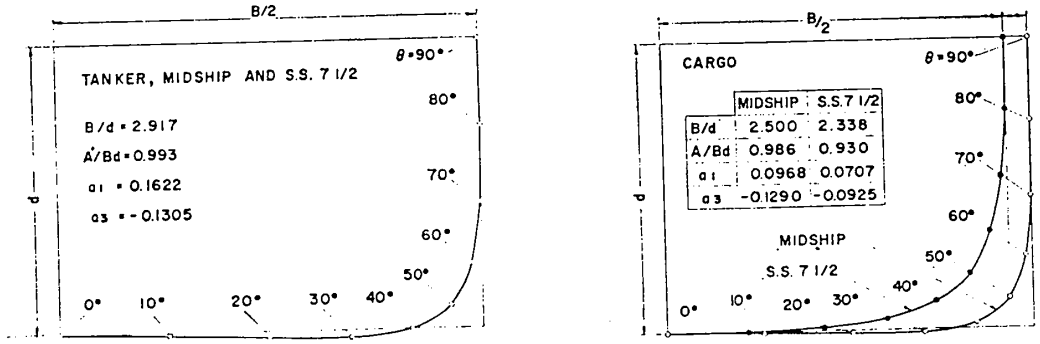

(a) (b)

Fig. 3.3 Transverse Sections of the Ships.

Square Station 7½ of these ships whose transverse sections were shown in Fig. 3.3. Previously mentioned p_s, p_{b1} and p_{b2} are the pressures on the points of $\theta=90°$, $0°$, $50°$ respectively.

3.1 *Response Function of the Pressure*

Calculated response functions of the hydrodynamic pressures p_b and p_s are shown in Fig. 3.4. The abscissa is the dimensionless wave length $\sqrt{L/\lambda}$, where λ is the wave length, L the ship length. $|H(\omega)|$ is response amplitude of the pressure, and $C(\omega)$ in-phase component of the pressure with respect to the wave, and $Q(\omega)$ is out-of phase component. The response amplitude of the hydrodynamic pressure on the side $|H_s(\omega)|$ is nearly equal to unit in range of large value of $\sqrt{L/\lambda}$. In such range ship motions are very small, however, the hydrodynamic pressure on the bottom $|H_b(\omega)|$ is not so small. This seems to be due to orbital motion of wave particle.

Here it is noted that the response function of the pressure on the bottom $H_b(\omega)$ is mean of the pressure on the bottom center line $H_{b1}(\omega)$ and on the bilge part:

$$H_b(\omega)=\frac{1}{2}\{H_{b1}(\omega)+H_{b2}(\omega)\}$$
$$=\frac{1}{2}\{C_{b1}(\omega)+C_{b2}(\omega)\}$$
$$+\frac{i}{2}\{Q_{b1}(\omega)+Q_{b2}(\omega)\} \quad (3.12)$$

ISSC spectrum given by the following equation was used to calculate $2S_w(\omega)$:

$$[f(\omega)]^2=0.11\,H^2\omega_1^{-1}\left(\frac{\omega}{\omega_1}\right)^{-5}$$
$$\cdot\exp\left\{-0.44\left(\frac{\omega}{\omega_1}\right)^{-4}\right\} \quad (3.13)$$
$$\omega_1=\frac{2\pi}{T}$$

where H is the significant wave height, T the average wave period. Curves of $[f(\omega)]^2/H^2$ are shown in Fig. 3.5.

3.2 *Correlation Coefficient of the Pressures on the Side and the Bottom*

In Fig. 3.6 are shown calculated results of standard deviation, R_s and R_b, of the hydrodynamic pressure on the side and on the bottom of previously mentioned ship forms, using the ISSC spectrum and the response function shown in Section 3.1. The abscissa in the average wave period T of the sea. The standard deviation R is shown in the dimensionless form $R/\gamma H$, where γ is weight of water per unit volume. This dimensionless value $R/\gamma H$ means that the standard deviation of the hydrodynamic pressure at the sea having unit significant wave height.

Observing the calculated response functions, it is reasonable that the standard deviation of the hydrodynamic pressure on the ship side is larger than that on the bottom, and the standard deviation of the pressure at S.S. 7½ is larger than that at the midship.

In Fig. 3.7 are shown calculated results of the correlation coefficients of the pressure on the side p_s and on the bottom p_b in long-created irregular head seas. From Fig. 3.7

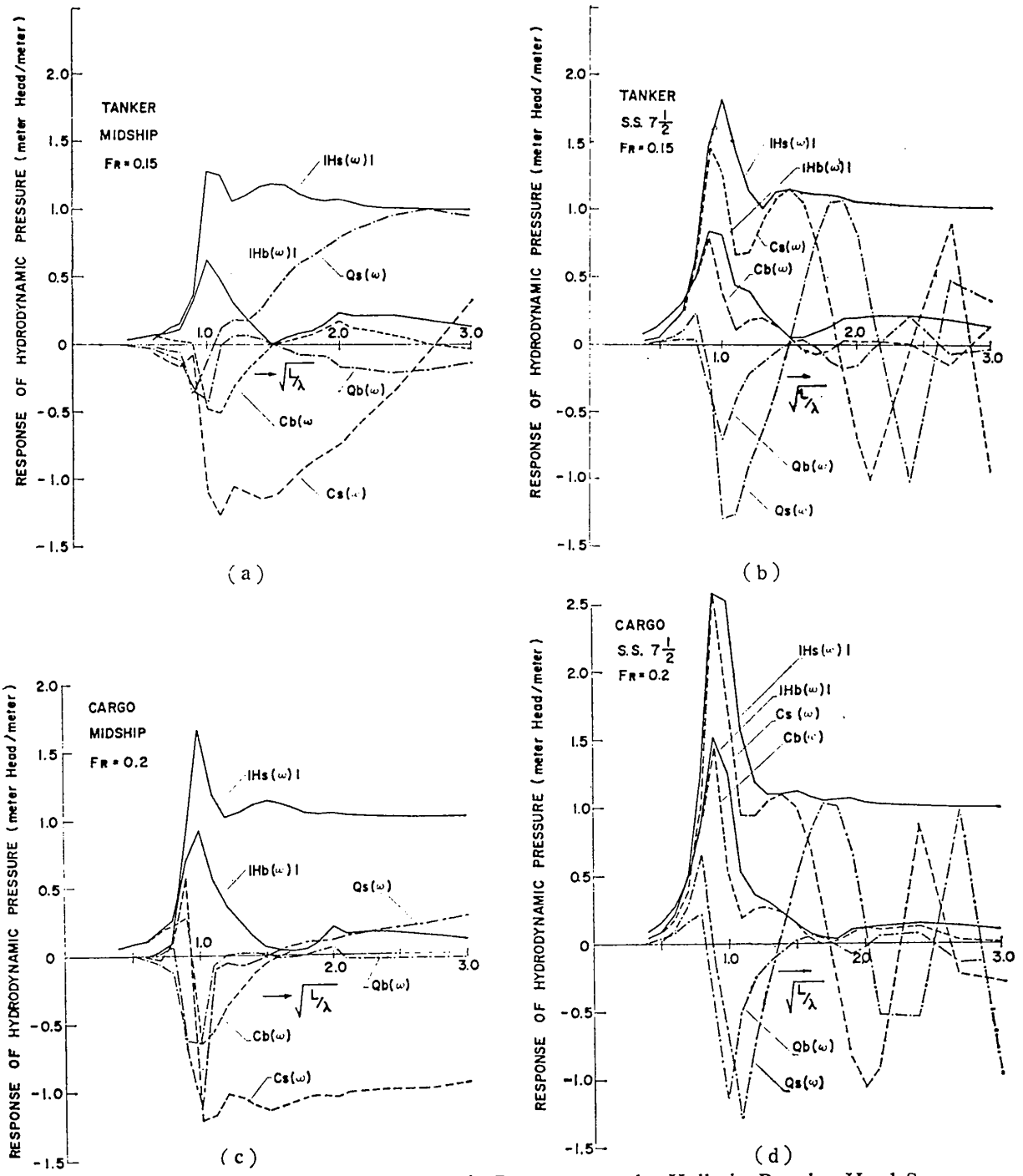

Fig. 3.4 Responses of the Hydrodynamic Pressures on the Hulls in Regular Head Seas.

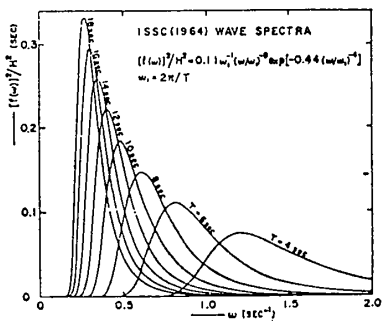

Fig. 3.5 ISSC Wave Spectra (from Ref. (16)).

it is noted that at the certain value of average wave period correlation coefficient ρ changes suddenly from minus to plus, and in rang above that average wave period ρ is almost constant. Fig. 3.8 shows change of ρ against ship speed for the 150 m cargo ship and the 300 m tanker. It will be seen that ρ slightly increase with ship speed.

The joint probability distributions (Eq. (3.1)) of the pressure on the side $p_s(t_1)$ and on

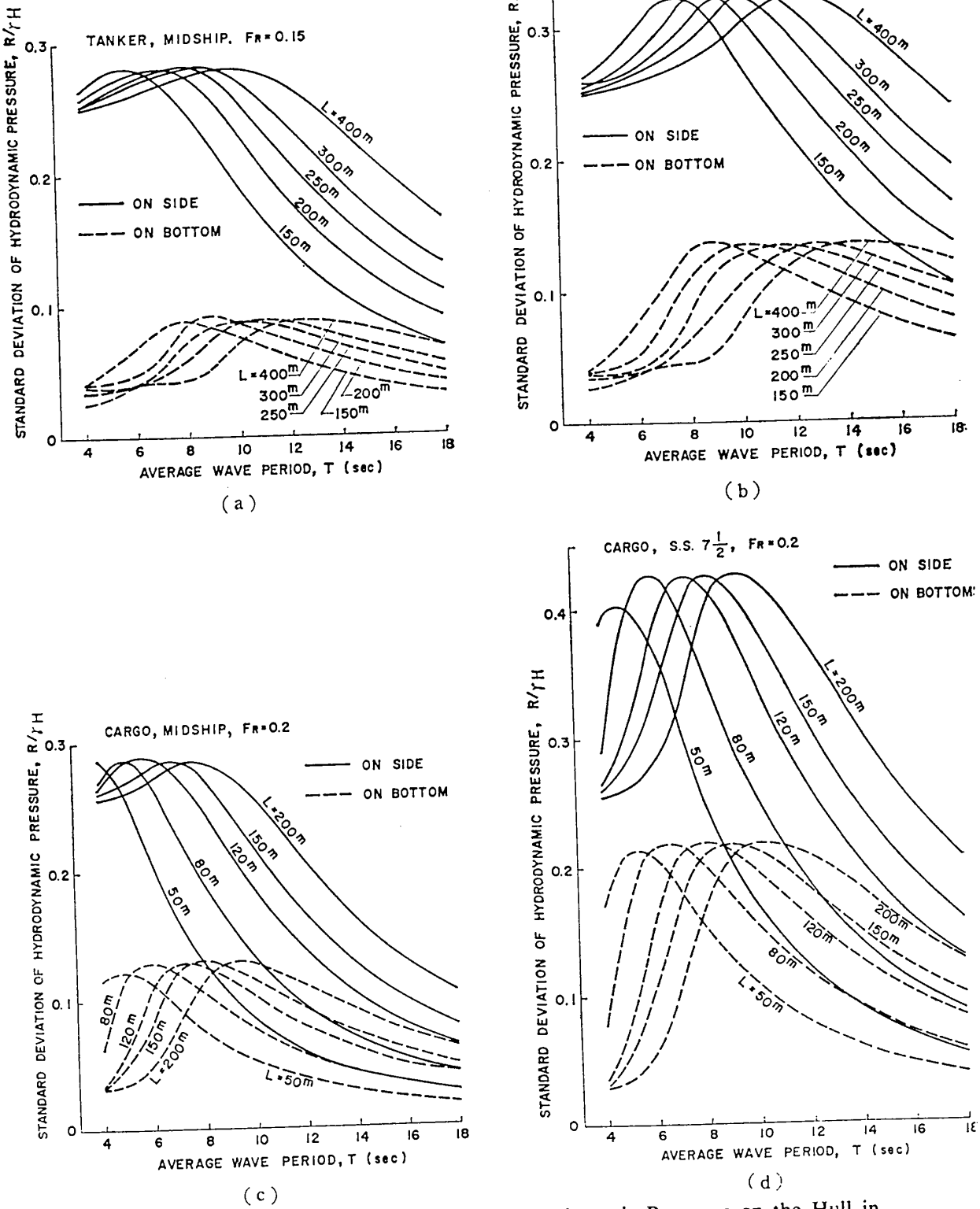

Fig. 3.6 Standard Deviations of the Hydrodynamic Pressures on the Hull in Long-Crested Irregular Head Seas.

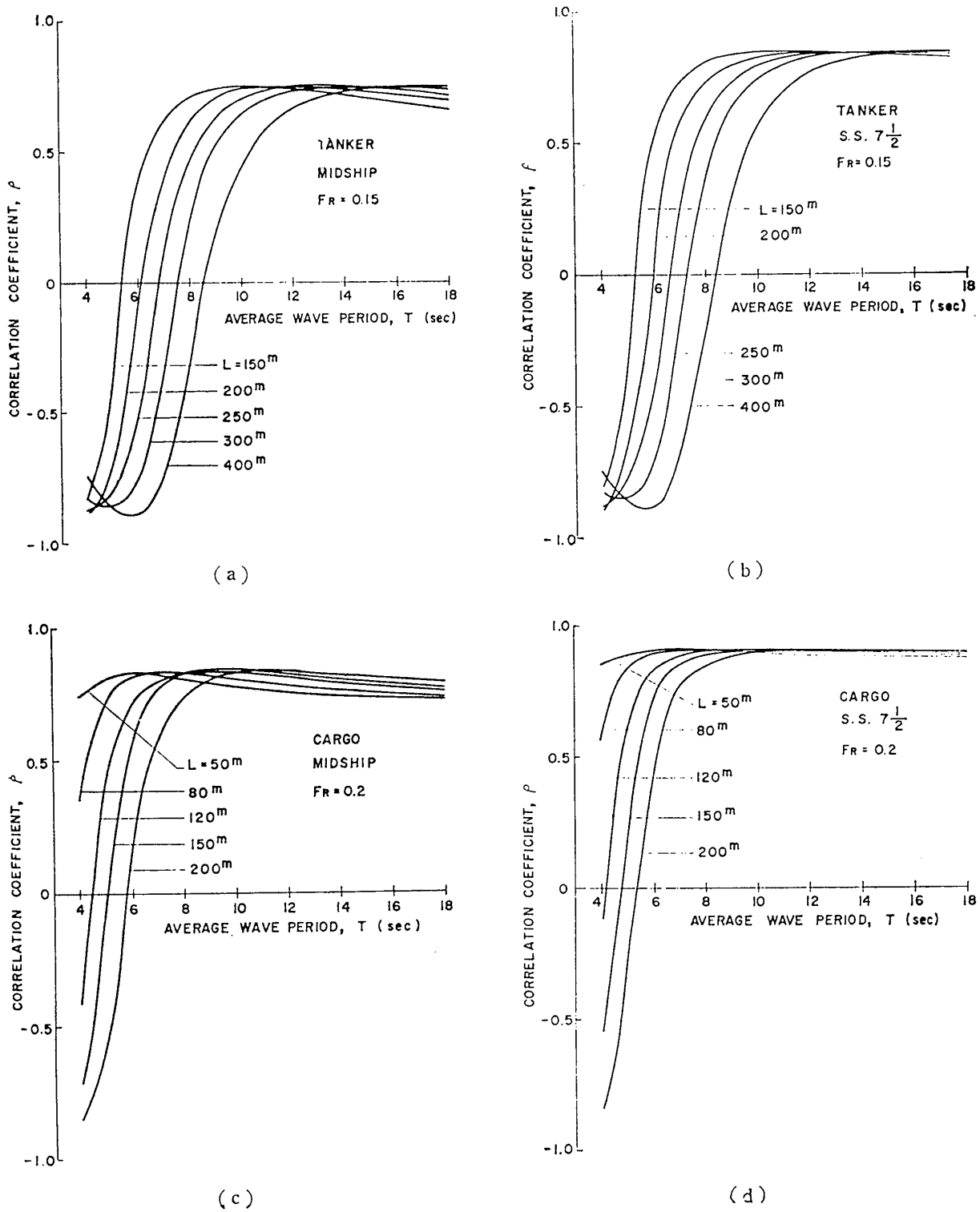

Fig. 3.7 Correlation Coefficients of P_s and P_b, in Long-Crested Irregular Head Seas.

P_s=The Hydrodynamic Pressure on the side.
P_b=The Hydrodynamic Pressure on the Bottom of the Hull.

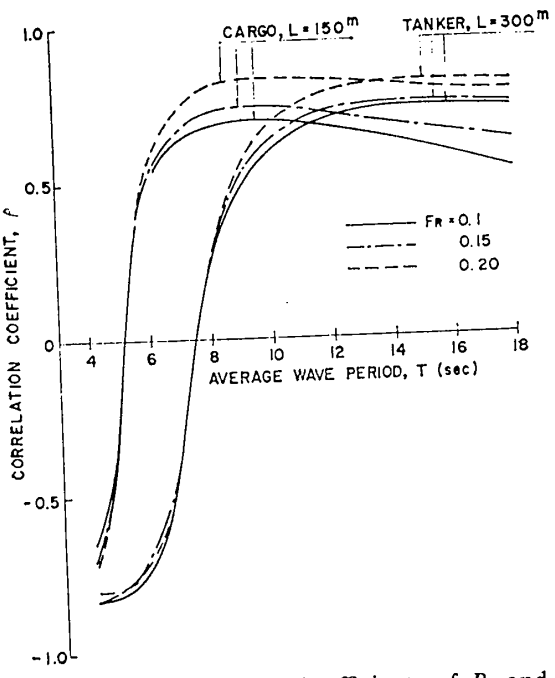

Fig. 3.8 Correlation Coefficients of P_s and P_b at Various Ship Speeds.

the bottom $p_b(t_1)$ of the cargo ship and the tanker are determined by the above-calculated value of R_s, R_b and ρ. When the hydrodynamic pressure on the side at $t=t_1$ is $p_s(t_1)$, the probability distribution of the pressure on the bottom $p_b(t_1)$ is given by

$$h\{p_b(t_1)\,|\,p_s(t)=p_s(t_1)\}=\frac{1}{R_b\sqrt{2\pi(1-\rho^2)}}e^{-\frac{1}{2}\phi} \tag{3.14}$$

$$\phi=\frac{1}{R_b(1-\rho^2)}\left\{p_b(t_1)-\frac{R_b\rho}{R_s}p_s(t_1)\right\} \tag{3.15}$$

From above probability function the following equation which gives mean value of $p_b(t_1)$ for the condition $p_s(t)=p_s(t_1)$:

$$p_b(t_1)=\frac{R_b p}{R_s}p_s(t_1) \tag{3.16}$$

Graphs of Eq. (3.17) for the 150 m cargo ship and the 300 m tanker are shown in Fig. 3.9. It can be seen that the expected values of the pressure on the bottom for the given value of the pressure on the side are about $0.5\,p_b(t_1)$ for the cargo ship, $0.3\,p_b(t_1)$ for the tanker in the range above certain value of average wave period; those are $-0.1\,p_b(t_1)$ in the range of small average wave period.

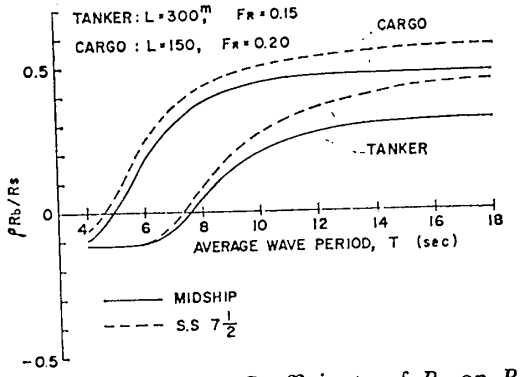

Fig. 3.9 Regression Coefficients of P_b on P_s, in Long Crested Irregular Head Seas.

P_b=The Hydrodynamic Pressure on the Bottom.
P_s=The Hydrodynamic Pressure on the Side of the Hull.

4. Conclusion

Distribution of the irregularly changing hydrodynamic pressure along the girth in long-crested irregular waves was studied in statistical means for the typical ship forms of the cargo ship and the tanker. Namely, spacial distribution of the pressure along the girth was represented by the pressures on the side on still water line and on the bottom. And the joint probability distribution of these two pressures for those ship forms was calculated.

The following conclusions were obtained:

(1) Correlation coefficients of the hydrodynamic pressures on the ship side and on the bottom are constant in the range of the average wave period which is larger than certain value, and those constant value of correlation coefficient is about 0.6 to 0.9. For small value of average wave period, correlation is minus.

(2) Expected values of the hydrodynamic pressure on the bottom for the given value of the pressure on the side are about 50% of the given bottom pressure for the cargo ship, about 30% for the tanker in the range above certain value of average wave period; those are about 10% in minus sign in the range of small average wave period.

Acknowledgements

The author wishes to express his thanks to Prof. J. Fukuda and Prof. F. Tasai for

guidance as well as for supplying data, and to Mr. N. Shimada for much help in carrying out the works. Mr. Kitagawa and staffs of Mejiro No. 1 Tank and of meguro Model Basin lent their cheerful collaboration to the experiments.

References

1) Y. AKITA, and K. OCHI: Investigations on the Strength of Ships Going in Waves by Model Experiments, J.S.N.A. Japan. Vol. 95, 1954, (in Japanese).
2) R. TASAKI, and Y. TAKEI: On the Measurements of the Hydrodynamic Pressure on the Bottom of a Ship by Ship Model Experiments in Waves, the 22nd Meeting of T.T.R.I. 1961, (in Japanese).
3) W. R. PORTER: Pressure Distributions, Added-Mass, and Damping Coefficients for Cylinders Oscillating in a Free Surface, Institute of Engineering Research, Univ. of California, Series No. 82, Issue No. 16, 1960.
4) J. R. PAULLING, and R. K. RICHARDSON: Measurement of Pressures, Forces, and Radiating Waves for Cylinders Oscillating in a Free Surface, Institute of Engineering Research, Univ. of California, Series No. 82, Issue No. 23, 1962.
5) H. HUANG: Measurement of Pressures and Hydrodynamic Forces on a Shiplike Model Oscillating in a Free Surface, Institute of Engineering Research, Univ. of California, NA-65-1, 1965.
6) D. HOFFMAN: Hydrodynamic Pressure Distribution on a Ship Hull in Waves, Contribution to the 11th ITTC, Seakeeping Committee, 1966.
7) F. B. BULL, and J. F. BAKER: Measurement and Recording of the Forces Acting on a Ship at Sea, Trans. I.N.A. Vol. 91, 1949.
8) The 10th and the 24th Research Committees: Experiments on the Strength of Ships in Rough Seas, Report of the Shipbuilding Research Association of Japan, No. 24, 1958, (in Japanese).
9) J. FUKUDA: On the Midship Bending Moments of a Ship in Regular Waves, J.S.N.A. Japan. Vol. 110, 1961.
10) G. VOSSERS, and W. A. SWAAN: Some Seakeeping Tests with a Victory Model, I.S.P. Vol. 7, No. 69, 1960.
11) Y. WATANABE: On the Theory of Heaving and Pitching Motions of a Ship, Technology Reports of the Kyushu Univ. Vol. 31, No. 1, 1958, (in Japanese).
12) F. Tasai: Damping Force and Added Mass of Ships Heaving and Pitching (Continued), Report of Research Institute for Applied Mechanics, Kyushu Univ. Vol. 8, No. 31, 1960.
13) F. TASAI: An Approximate Calculation of Hydrodynamic Pressure on the Midship Section Contour of a Ship Heaving and Pitching in Regular Waves, Report of Research Institute for Applied Mechanics, Kyushu Univ. Vol. 14, No. 48, 1966.
14) K. GODA: Hydrodynamic Pressure on a Midship in Waves, J.S.N.A. Seibu. Japan. No. 35, 1968, (in Japanese).
15) F. TASAI: On the Damping Force and Added Mass of Ships Heaving and Pitching, Reports of Research Institute for Applied Mechanics, Kyushu Univ. Vol. 7, No. 16, 1959.
16) J. FUKUDA: Trends of Extreme Wave Bending Moment According to Long-Term Predictions, J.S.N.A. Japan. Vol. 123, 1968 (in Japanese).